Original Article

JOURNAL OF COMPOSITE MATERIALS

Journal of Composite Materials
0(0) 1–8

DOI: 10.1177/0021998312473860
jcm.sagepub.com

SAGE

Study on the synthesis and properties of polyacrylamide/Na-montmorillonite nanocomposites

Zafer Koç[1], Meltem Çelik[2], Müşerref Önal[2], Yüksel Sarıkaya[2], Yağmur Öner[3] and Leyla Açık[3]

Abstract

A series polyacrylamide/Na-montmorillonite nanocomposites was prepared by in situ free radical polymerization in aqueous medium using benzoyl peroxide (Bz_2O_2) as a radical initiator. To characterize the resultant nanocomposites, Fourier transform infrared spectroscopy, X-ray diffraction, scanning electron microscopy, transmission electron microscopy, and thermogravimetric analysis techniques were used. The moisture retain, water uptake, antibacterial properties, BET specific surface area and specific nanopore volume of nanocomposites were determined. The X-ray diffraction pattern showed that the polyacrylamide was intercalated up to 60.0 mass% acrylamide concentration, and then montmorillonite layers exfoliated into the polyacrylamide matrix. The interlayer spacing (d_{001}) of the montmorillonite increased from 1.19 to 1.90 nm by intercalation. Transmission electron microscopy views showed that the Na-montmorillonite partially exfoliated in polyacrylamide. The nanocomposites exhibited better thermal stability than the pure polyacrylamide.

Keywords

Nanocomposites, clay, polyacrylamide, montmorillonite, benzoyl peroxide, in situ free radical polymerization

Introduction

Polymer/clay nanocomposites have been studied extensively in recent years.[1–4] Clays are inorganic layered materials of relatively low cost, abundant, and have excellent chemical and thermal resistance for synthesis of polymer/clay nanocomposite. Among the many layered materials, the montmorillonite (MMT) is one of the widely used silicate minerals.

Compared to pure polymers, polymer/clay nanocomposites exhibit enhanced mechanical properties, thermal stability, and gas-barrier properties.[5–7]

Among the monomers, acrylamide (AAm) has been widely applied as vinyl monomer for commercial applications. It is highly water soluble, polar and less expensive than other vinyl monomers. It is one of the most important vinyl monomers because of the hydrophilic nature of the AAm. The polymerization of hydrophilic polymer such as polyacrylamide (PAAm) also improves the antibacterial properties.[8,9]

Therefore, the aim of this article is to improve the thermal stability of PAAm through the synthesis with layered materials such as clay. During this method, the thermal properties of polymers in composite form is improving with incorporating clay.

Although many papers on polymer/modified clay nanocomposites were available in the literature,[10–12] there is little work about preparation, characterization, and properties of PAAm/unmodified Na-MMT nanocomposites synthesized by in situ polymerization. Therefore, this article describes new types of nanocomposites, PAAm, and unmodified Na-MMT. AAm was polymerized by an in situ polymerization in the presence of unmodified Na-MMT. The structure and some properties of the resulting polymer nanocomposites were characterized.

[1]Graduate School of Natural and Applied Sciences, Ankara University, Turkey
[2]Department of Chemistry, Faculty of Science, Ankara University, Turkey
[3]Department of Biology, Faculty of Science, Gazi University, Turkey

Corresponding author:
Meltem Çelik, Department of Chemistry, Faculty of Science, Ankara University, 06100 Tandoğan, Ankara, Turkey.
Email: mecelik@science.ankara.edu.tr

Experimental

Materials

Reagent grade AAm (Merck) was used without further purification. A free radical initiator, benzoyl peroxide (Bz_2O_2) (Merck) was twice purified by recrystallization from methanol (Merck) and chloroform (Merck) mixture. Sodium MMT (Na-MMT) was provided from Reşadiye (Tokat/Turkey) bentonite clay. It has a cation exchange capacity of 108 meq/100 g of clay, and was used after further purification.[13] The chemical composition of the Na-MMT in mass percent was: 61.37% SiO_2, 15.69% Al_2O_3, 3.56% Fe_2O_3, 0.94% CaO, 2.00% MgO, 1.96% Na_2O, 0.33% K_2O, 0.31% TiO_2, and 11.33% loss on ignition, which was determined by atomic absorption spectrometry. Its specific surface area is 51.24 m^2/g, and its X-ray diffraction (XRD) analysis shows that the interlayer spacing of Na-MMT is 1.19 nm. All other chemicals were analytical grade. AAm has great water absorption affinity.

Synthesis of nanocomposites

Na-rich MMT was obtained, as previously described in the literature Onal et al.,[13] by the methods of dispersion and sedimentation from its aqueous suspension. A series of PAAm/Na-MMT nanocomposites were synthesized using in situ free radical polymerization in aqueous medium according to the following procedure.[14]

Na-MMT (1 g) was dispersed in 23 mL of distilled water in a 100 mL Pyrex glass tube and was stirred at a rate of 100 r/min in overnight at room temperature for each polymerization. The AAm and the aqueous Na-MMT suspension were mixed with the different mass ratios as presented in Table 1. The Bz_2O_2 solution in acetone (3.75×10^{-3} mol/L) was added as 1 mL to the prepared mixtures. The obtained mixtures were polymerized in water bath (Lauda D40 S, Germany) at 85°C for 3 h to synthesize the PAAm/Na-MMT composites. Then, composites were dried in a vacuum oven at 50°C and weighed. Additional samples were prepared following the same conditions using different quantities of AAm.

Examination of prepared nanocomposites

The infrared spectra of samples in the form of KBr pellets were done with a Perkin Elmer 100 Model Fourier transform infrared spectroscopy (FT-IR) spectrophotometer in the range 450–4000 cm^{-1}.

XRD patterns of the Na-MMT and prepared nanocomposites were obtained with an Inel Equinox 1000 powder diffractomer, using Co-Kα radiation ($\lambda = 0.178901$ nm) ranging from 2° to 20°.

Table 1. Data on polymerization and chemical formation in PAAm and Na-MMT system[a].

Sample code	Monomer content (mass %)
PAAm/Na-MMT 1	33.3
PAAm/Na-MMT 2	50.0
PAAm/Na-MMT 3	60.0
PAAm/Na-MMT 4	66.7
PAAm/Na-MMT 5	71.4
PAAm/Na-MMT 6	75.0

PAAm: polyacrylamide; MMT: montmorillonite.
[a]$[Bz_2O_2]$: 3.75×10^{-3} mol/L, temperature: 85°C, time: 3 h.

The thermal stability of the materials was determined using a Shimadzu simultaneous differential thermal analyzer (DTA)–TG apparatus (DTG-60H Model) thermal analyzer under a 200 mL/min flow of nitrogen atmosphere at a heating rate 10°C/min from room temperature to 1000°C and α-Al_2O_3 was used as an inert material.

The morphology of nanocomposites was observed using a SEM-Zeiss EVO40 Model scanning electron microscope (SEM) with at an accelerating voltage of 30 kV. All samples were coated with gold prior to analysis.

The microstructure of nanocomposites was observed using a TEM-FEI Tecnai G2 transmission electron microscope (TEM) with at an accelerating voltage of 120 kV. The samples embedded in epoxy resin were microtomed with a Leica ultracut-R. Ultrathin sections were cut with a glass knife and deposited on one layer of carbon 300 mesh copper grids prior to analysis.

The BET specific surface area and specific nanopore volume of Na-MMT and nanocomposites were determined from nitrogen adsorption/desorption data at liquid nitrogen temperature, measured the Quantachrome NOVA 2200 surface area and pore size analyzer. The samples were outgassed at 150°C for 4 h under vacuum of 10^{-3} mmHg before the adsorption experiments.

The weighed dry samples in the form of pellet were conditioned at 25°C in medium having 100% humidity for 24 h for the moisture retain measurements. The percentage moisture retain was calculated from the difference between the masses of the conditioned and unconditioned samples (i.e. moisture retain% $= (M_2 - M_1)/M_1 \times 100$, where M_2 and M_1 are the masses of the conditioned and unconditioned samples, respectively).[2,15]

The dry samples in the form of pellet were weighed, M_1 and then kept in distilled water for 2 h at 25°C. After immersion, the wet samples were wiped using

filter paper and reweighed immediately, M_2. The percentage water uptake of samples was determined from using formula $(M_2 - M_1)/M_1 \times 100$.[2,14,15]

Antibacterial properties of the PAAm/Na-MMT nanocomposites were verified by testing in vitro with different bacteria species. *Bacillus cereus, Staphylococcus aureus, Pseudomonas aeruginosa,* and *Escherichia coli* (35218) were used to evaluate the antibacterial activity by disc diffusion method.[16,17] Nanocomposites were cut to make disc for measurement of antibacterial activity. In this method, inoculums of bacteria was prepared in 0.85% saline using McFarland standard and inoculated uniformly on nutrient agar plates. The disc was placed on the agar surface of the plate. The zone of inhibition for each nanocomposites was measured after overnight incubation at 37°C. If the bacteria are susceptible to a particular compound, an area of clearing surrounds the wafer where bacteria are not capable of growing (called a zone of inhibition).

Results and discussion

X-ray diffraction

XRD patterns for the hydrous Na-MMT, pure PAAm, and a series of PAAm/Na-MMT nanocomposites with different AAm monomer content appear in Figure 1(a) to (h). It can be observed from Figure 1(a) that the hydrous Na-MMT exhibits a characteristic crystalline peak at $2\theta = 8.6°$, corresponding to a d_{001} spacing of 1.19 nm. The XRD pattern of the nanocomposites showed that the characteristic crystalline peak was shifted toward lower angles for the nanocomposites due to the intercalation of AAm between the Na-MMT layers (Figure 1(b) and (c)). Using Bragg's equation ($d = n\lambda/2\sin\theta$), the d_{001} spacing values of the samples were calculated and used to characterize the layered structure of the nanocomposites. As shown in Figure 1(b) and (c), the average Na-MMT interlayer distance shifted from 1.19 to 1.90 nm up to 60.0% monomer content. These results indicate and support that the formation of intercalated and partially exfoliated nanocomposites with higher interlayer spacing. On the other hand, no significant peak was found for PAAm/Na-MMT nanocomposites as amount of the AAm content increases from 60.0 to 75.0%, which means that the Na-MMT layers (Figure 1(d) to (g)) are exfoliated.[18,19] The peak at $2\theta = 10°$ was originated from anhydrous Na-MMT. It was formed after losing interlayer water of hydrous Na-MMT. This water absorbed by the hydrophilic AAm. Gradual decrease in intensity of this peak by increasing by the AAm content showed that the anhydrous Na-MMT exfoliated harder the hydrous one.

FT-IR spectroscopy

The structure of PAAm/Na-MMT nanocomposite has been confirmed by comparing the IR spectra of Na-MMT and pure PAAm. Figure 2(a) to (c) shows the FT-IR spectra of Na-MMT, pure PAAm, and PAAm/Na-MMT6 nanocomposite. The characteristic peaks of Na-MMT at 1040 cm^{-1} (Si–O), 525 cm^{-1} (Al–O), 470 cm^{-1} (Mg–O), and 3630 and 3525 cm^{-1} (O–H stretching) is observed in the spectra Figure 2(a) and the characteristic peaks of PAAm at 3206 and 3362 cm^{-1} (N–H stretching) as broad single peak, 1668 cm^{-1} (CO amide), and 1620 cm^{-1} (C–N resonance) is observed in the spectra (Figure 2(c)). The peaks identified are consistent with previously published data.[3,14,20] The absence of the IR absorption peak for the Na-MMT on the nanocomposite sample showed the exfoliation of MMT plates in PAAm polymer. This spectra is in agreement with the XRD result.

Scanning electron microscopy

The distribution of the Na-MMT layers in the polymer matrix was studied with SEM. Figure 3(a) and (b) shows SEM micrographs of the Na-MMT and PAAm/Na-MMT4 nanocomposite. These figures showed the difference between surfaces morphologies of the natural clay mineral and one of the composites. It can be observed from Figure 3(a) that a sheet-like plates of the clay. After polymerization, the nanocomposite shows significant changes in morphology (Figure 3(b)). It can be seen that PAAm polymerization occurred within the Na-MMT layers and a satisfactory dispersion of clay layers in the polymer matrix. This morphological pattern was also observed by other researchers.[21,22]

Transmission electron microscopy

To further confirm the morphology of the nanocomposites, TEM was used. The TEM micrograph of PAAm/Na-MMT2 nanocomposite is shown in Figure 4. The light areas represent the polymer matrix while the darker lines represent individual MMT layers in the micrograph. TEM image of PAAm/Na-MMT2 nanocomposite shows that individual layers of the Na-MMT are well dispersed in the PAAm matrix and separated one from the other and most of the Na-MMT layers have exfoliated as pointed in the figure. Some agglomeration of clay platelets was observed. This micrograph is in agreement with the XRD result. This feature was similar to the observations of other researchers.[23,24]

Thermal properties

Figure 5 (a) to (d) shows curves for thermogravimetric analysis (TGA) measurements used to determine mass

loss due to thermal degradation of Na-MMT, pure PAAm, PAAm/Na-MMT2, and PAAm/Na-MMT6. The TGA curve of Na- MMT indicates that there are two decomposition steps (Figure 5(a)). The first minor mass loss step lower than 125°C was due to removal of moisture and absorbed water. The second major mass loss step when the temperature is higher 800°C was the water resulting from the structural –OH groups of Na-MMT begins to be removed. The total mass loss is only 19.8% up to 1000°C. As could be expected, the Na-MMT shows a high thermal stability.[7]

As shown in Figure 5(b), it is a small mass loss (~11.47%) just below 160°C is attributed to the loss of absorbed water of pure PAAm. The decomposition of the pure PAAm began at 230°C, and completed of 100% at 1000°C, which was attributed to thermal decomposition of the PAAm chains. Consequently, pure PAAm should exhibit lower thermal stability relative to Na-MMT.

For the nanocomposites, the PAAm/Na-MMT2 has a higher decomposition temperature (300°C) which is 70°C more than that of pure PAAm, and exhibited a mass loss of 54.9% at 1000°C. It is a small mass loss (~7.5%) just below 160°C is attributed to the loss of absorbed water (Figure 5(c)). But, with the AAm content further increased to 75.0 mass% (PAAm/Na-MMT6) has a lower decomposition temperature (270°C) and exhibited a mass loss of 76.5% at 1000°C than 50.0 mass% AAm containing nanocomposite (PAAm/Na-MMT2) because the clay content is low in this sample. Similarly, a small mass loss (~8.6%) just below 160°C is attributed to the loss of absorbed water (Figure 5(d)). Evidently, incorporation of PAAm with Na-MMT would be expected to enhance the

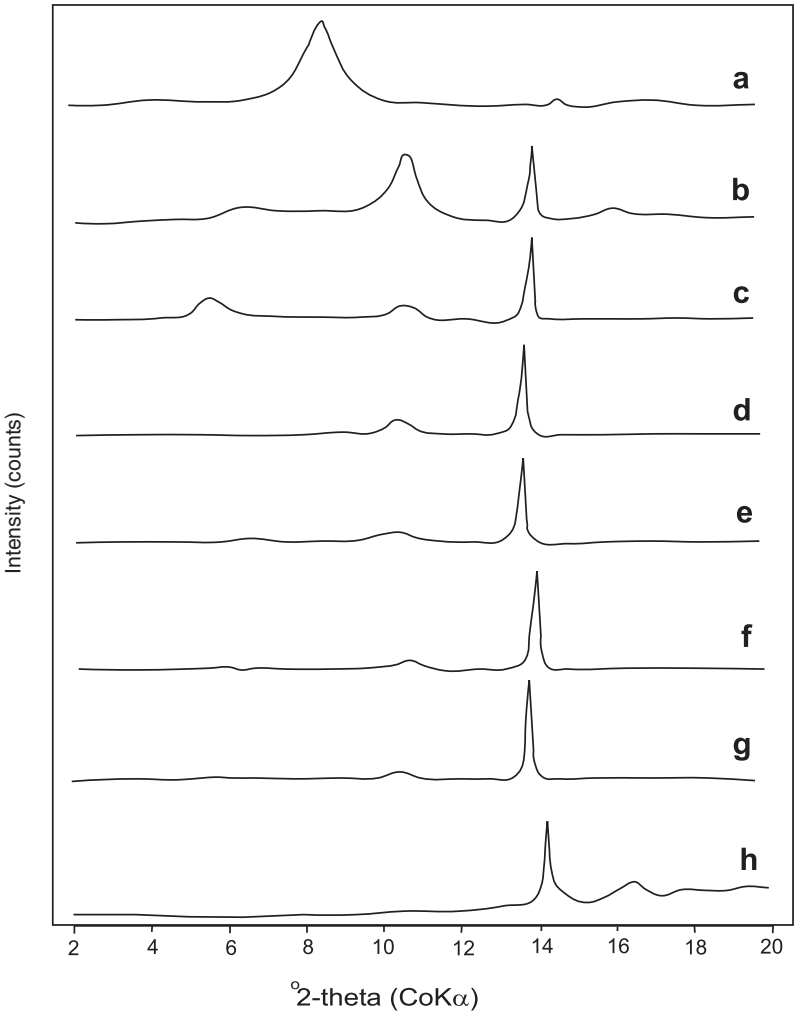

Figure 1. XRD patterns of (a) Na-MMT, (b) PAAm/Na-MMT1, (c) PAAm/Na-MMT2, (d) PAAm/Na-MMT3, (e) PAAm/Na-MMT4, (f) PAAm/Na-MMT5, (g) PAAm/Na-MMT6, and (h) PAAm.
XRD: X-ray diffraction; MMT: montmorillonite; PAAm: polyacrylamide.

thermal stability of PAAm/Na-MMT2 and PAAm/Na-MMT6 nanocomposites relative to that of pure PAAm. This enhances thermal stability of the PAAm/Na-MMT nanocomposites is due to Na-MMT acts as barrier to heat flow. These views are consistent with the observed trend.[25–28]

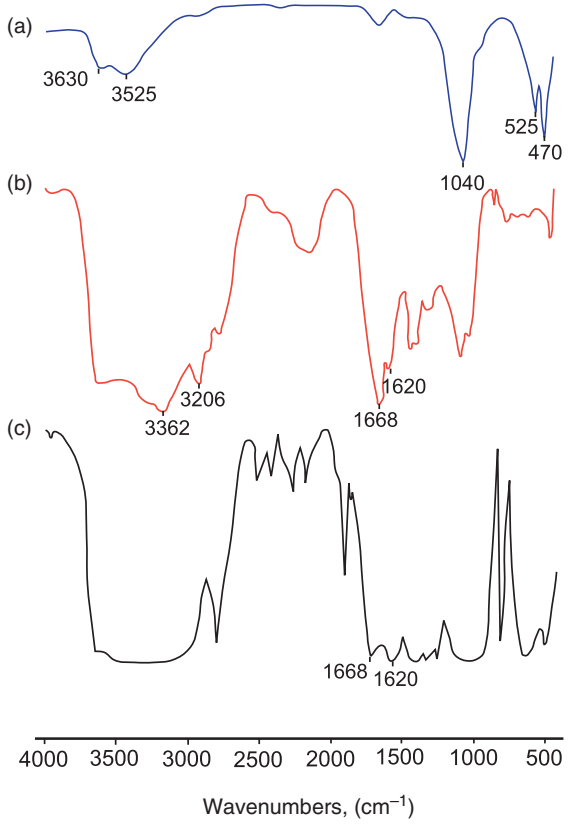

Figure 2. FT-IR spectra of (a) Na-MMT, (b) pure PAAm, and (c) PAAm/Na-MMT6 nanocomposite.
FT-IR: Fourier transform infrared spectroscopy; MMT: montmorillonite; PAAm: polyacrylamide.

The BET surface areas and nanopore volume

The BET surface areas and nanopore volumes of Na-MMT and PAAm/Na-MMT nanocomposites were determined using the NOVA surface area analyzer and presented in Table 2.

As could be expected, the Na-MMT shows the higher than BET surface area and nanopore volume than PAAm/Na-MMT nanocomposites. BET surface area and nanopore volume of Na-MMT were $51.24\,m^2g^{-1}$ and $0.078\,cm^3g^{-1}$, respectively. One can see that these values dramatically went down to $1.51\,m^2g^{-1}$ and $0.009\,cm^3g^{-1}$ for PAAm/Na-MMT2, and $0.90\,m^2g^{-1}$ and $0.008\,cm^3g^{-1}$ for PAAm/Na-MMT3, respectively. This could be explained in terms of covering or filling of the pores by PAAm.[2,20,29] Nitrogen adsorption capacity as well as specific surface

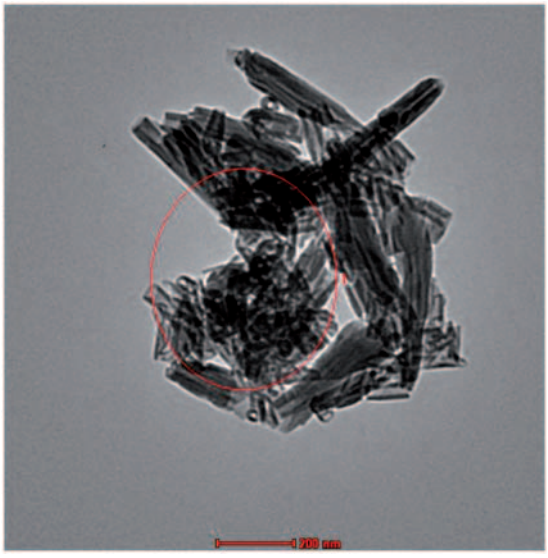

Figure 4. TEM image of PAAm/Na-MMT2 nanocomposite.
TEM: transmission electron microscope; MMT: montmorillonite; PAAm: polyacrylamide.

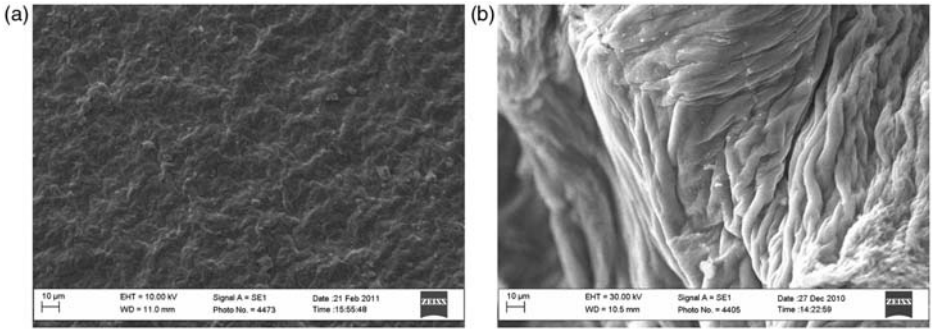

Figure 3. SEM images of (a) Na-MMT and (b) PAAm/Na-MMT4 nanocomposite.
SEM: scanning electron microscopy; MMT: montmorillonite; PAAm: polyacrylamide.

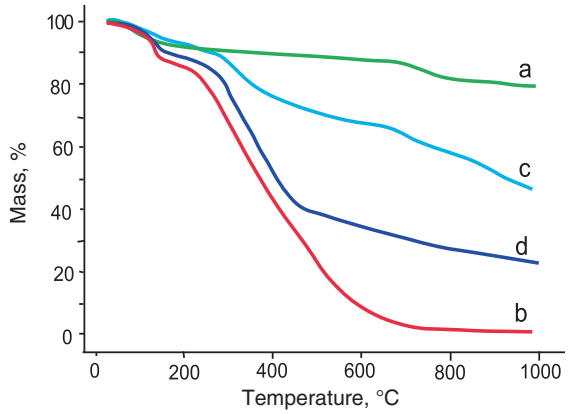

Figure 5. TGA curves of (a) Na-MMT, (b) pure PAAm, (c) PAAm/Na-MMT2, and (d) PAAm/Na-MMT6 nanocomposite obtained in nitrogen atmosphere at heating rate of 10°C/min.
TGA: thermogravimetric analysis; MMT: montmorillonite; PAAm: polyacrylamide.

Table 2. The BET specific surface areas (*A*) and specific nanopore volumes (*V*) of the Na-MMT and PAAm/Na-MMT nanocomposites.

Sample	*A* (m^2g^{-1})	*V* (cm^3g^{-1})
Na-MMT	51.24	0.078
PAAm/Na-MMT 2	1.51	0.009
PAAm/Na-MMT 3	0.90	0.008

MMT: montmorillonite; PAAm: polyacrylamide.

area and specific pore volume decreased due to the dissappearing of nanoporosity of the Na-MMT by the exfoliation.

Properties of PAAm/Na-MMT nanocomposites

Moisture retains and water uptake measurements. The percentage moisture retains and water uptake values of Na-MMT and PAAm/Na-MMT nanocomposites with increasing AAm content are shown in Figures 6 and 7. It was observed that moisture retain gradually, but water uptake of nanocomposites remarkably decreased.

The decreases in moisture retain and water uptake can be attributed to the percentage of clay in the composites being limited, which reflects that the quantity of the polymer introduced in the layers reaches a limit and is enough to achieve maximum opening of the interlayers of clay and the formation of a cross-linked structure to a certain extent which prevents the insert on of water molecules. Finally, water resistance of these composites which as defined the decreases in moisture retain and water uptake values can be greatly improved.[2,14]

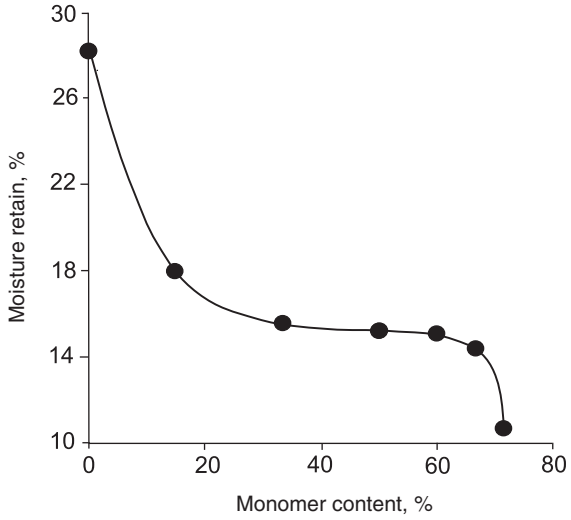

Figure 6. The percentage moisture retain values of Na-MMT and PAAm/Na-MMT nanocomposites obtained including different percentages of AAm.
MMT: montmorillonite; PAAm: polyacrylamide.

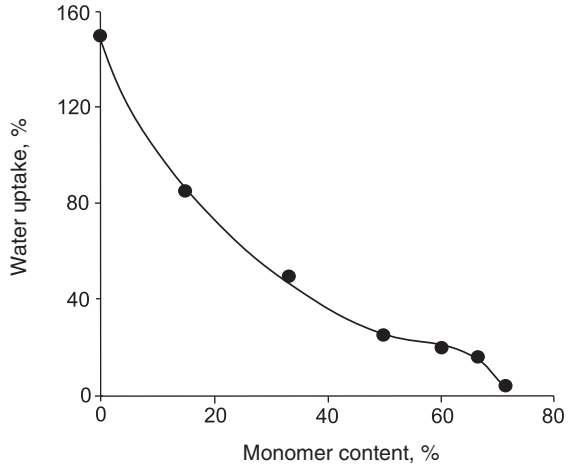

Figure 7. The percentage water uptake values of Na-MMT and PAAm/Na-MMT nanocomposites obtained including different percentages of AAm.
MMT: montmorillonite; PAAm: polyacrylamide.

Determination of antibacterial properties. Antibacterial activity for PAAm/Na-MMT nanocomposites were evaluated against *B. cereus, S. aureus, P. aeruginosa,* and *E. coli* (35218) strains. Disc diffusion technique was carried out and the zone of inhibition for different concentrations of nanocomposites were measured. All the nanocomposites exhibited good antibacterial activity against various pathogens bacterial strain particularly *P. aeruginosa*. The antibacterial activity of nanocomposites for *bacteria* was increased with AAm

Table 3. The antibacterial activity results of Na-MMT and PAAm/Na-MMT nanocomposites[a].

Tested bacteria	Sample	Measured the inhibition zone (mm)
Bacillus cereus	Na-MMT	16
	PAAm/Na-MMT 4	24
	PAAm/Na-MMT 6	29
Staphylococcus aureus	Na-MMT	16
	PAAm/Na-MMT 4	25
	PAAm/Na-MMT 6	35
Pseudomonas aeruginosa	Na-MMT	16
	PAAm/Na-MMT 4	40
	PAAm/Na-MMT 6	50
Escherichia coli (35218)	Na-MMT	16
	PAAm/Na-MMT 4	25
	PAAm/Na-MMT 6	30

MMT: montmorillonite; PAAm: polyacrylamide.
[a]Diameter of samples is 16 mm before experiment.

monomer content. Measured inhibition zones are presented in Table 3.

Conclusions

In this study, synthesis and characterization of PAAm/Na-MMT nanocomposites prepared by in situ free radical polymerization were successfully studied. The thermal property of nanocomposites was investigated by TGA. The resulting nanocomposites show more thermally stable than pure PAAm and Na-MMT clay induced the thermal stability. The overall thermal stability trends as follows: Na-MMT >PAAm/Na-MMT2 >PAAm/Na-MMT6 >pure PAAm was found, respectively. Intercalated, partially exfoliated, and exfoliated morphology observed for nanocomposites and proved by XRD results. XRD results reveal that interlayer distance of Na-MMT increased with AAm content up to 60.0 wt% and then no further increase of interlayer distance at higher AAm content was observed. The TEM image showed the Na-MMT partially exfoliated in PAAm. BET specific surface area, specific nanopore volume, moisture retains and water uptake values of composites obviously decreased compared with that of Na-MMT. Furthermore, antibacterial properties of nanocomposites were increased with AAm content.

Funding

The authors are grateful to the Turkish Scientific and Research Institute (project number 108T241) for their financial support to this study.

Declaration of interest

None declared.

References

1. Akat H, Taşdelen MA, Du Prez F, et al. Synthesis and characterization of polymer/clay nanocomposites by intercalated chain transfer agent. *Eur Polym J* 2008; 44: 1949–1954.
2. Çelik M and Önal M. Synthesis and characterization of poly(glycidyl methacrylate)/Na-montmorillonite nanocomposites. *J Appl Polym Sci* 2004; 94: 1532–1538.
3. Anbarasan R, Arvind P and Dhanalakshmi V. Synthesis and characterization of polymethacrylamide–clay nanocomposites. *J Appl Polym Sci* 2011; 121: 563–573.
4. Choi HJ, Kim JW, Joo J, et al. Synthesis and electrorheology of emulsion intercalated PANI-clay nanocomposite. *Synth Met* 2001; 121: 1325–1326.
5. Kumar S, Jog JP and Natarajan U. Preparation and characterization of poly(methyl methacrylate)–clay nanocomposites via melt intercalation: the effect of organoclay on the structure and thermal properties. *J Appl Polym Sci* 2003; 89: 1186–1194.
6. Çelik M, Önal M and Sarıkaya Y. Poly(methyl acrylate)/Na-montmorillonite intercalated composites: preparation and characterization. *J Appl Polym Sci* 2012; 123: 3662–3667.
7. Çelik M and Önal M. Synthesis, characterization, and properties of conducting polypyrrole/Na-montmorillonite nanocomposites. *J Thermoplast Compos* 2012; 25: 505–520.
8. Kenawy E-R, Abdel-Hay FI, Abou El-Magd A, et al. Synthesis and antimicrobial activity of some polymers derived from modified amino polyacrylamide by reacting it with benzoate esters and benzaldehyde derivatives. *J Appl Polym Sci* 2006; 99: 2428–2437.
9. Solovskii MV, Eropkin M Yu, Eropkina EM, et al. Complexes of aminoglycoside antibiotics with copolymers of acrylamide with acrylic and methacrylic acids. *Pharm Chem J* 2010; 44: 314–318.
10. Oral A, Shahwan T and Güler Ç. Synthesis of poly-2-hydroxyethyl methacrylate–montmorillonite nanocomposite via in situ atom transfer radical polymerization. *J Mater Res* 2008; 23: 3316–3322.
11. Jaymand M. Surface modification of montmorillonite with novel modifier and preparation of polystyrene/montmorillonite nanocomposite by in situ radical polymerization. *J Polym Res* 2011; 18: 957–963.
12. Nikolaidis A, Achilias D and Karayannidis G. Synthesis and characterization of PMMA/Organomodified montmorillonite nanocomposites prepared by in situ bulk polymerization. *Ind Eng Chem Res* 2011; 50: 571–579.
13. Önal M, Sarıkaya Y, Alemdaroğlu T, et al. Isolation and characterization of a smectite as a micro-mesoporous material from a bentonite. *Turk J Chem* 2003; 27: 683–693.
14. Önal M and Çelik M. Polymethacrylamide/Na-montmorillonite nanocomposites synthesized by free-radical polymerization. *Mater Lett* 2006; 60: 48–52.

15. Çelik M. Preparation and characterization of starch-g-polymethacrylamide copolymers. *J Polym Res* 2006; 13: 427–432.
16. Ekambaram R, Rathna D, Manian RS, et al. Synthesis and antibacterial property of quinolines with potent DNA gyrase activity. *Bioorg Med Chem* 2009; 17: 660–666.
17. Çelik M, Qudrat ML, Akyüz E, et al. Synthesis and characterization of acrylic fibers-g-polyacrylamide. *Fibers Polym* 2012; 13: 145–152.
18. Meneghetti P and Qutubuddin S. Synthesis of poly(-methyl methacrylate) nanocomposites via emulsion polymerization using a zwitterionic surfactant. *Langmuir* 2004; 20: 3424–3430.
19. Manzi-Nshuti C, Chen D, Su S, et al. Structure–property relationships of new polystyrene nanocomposites prepared from initiator-containing layered double hydroxides of zinc aluminum and magnesium aluminum. *Polym Degrad Stab* 2009; 94: 1290–1297.
20. Sur GS, Lyu SG and Chang JH. Synthesis and LCST behavior of thermosensitive poly(*N*-isopropylacrylamide)-clay nanocomposites. *J Ind Eng Chem* 2003; 9: 58–62.
21. Mészáros L and Czvikovszky T. Polyamide-6 nanocomposites with electron-beam-treated clay. *Radiat Phys Chem* 2007; 76: 1329–1332.
22. Çelik M and Önal M. Intercalated polyaniline/Na-montmorillonite nanocomposites via oxidative polymerization. *J Polym Res* 2007; 14: 313–317.
23. Han Y and Lu Y. Preparation and characterization of exfoliated organic montmorillonite/poly(3,4-ethyldioxythiophene) nanocomposites. *J Appl Polym Sci* 2009; 111: 2400–2407.
24. Hossain MD, Kim WS, Hwang HS, et al. Role of water on PMMA/clay nanocomposites synthesized by in situ polymerization in ethanol and supercritical carbon dioxide. *J Colloid Interface Sci* 2009; 336: 443–448.
25. Tiwari RR and Natarajan U. Thermal and mechanical properties of melt processed intercalated poly (methyl methacrylate)–organoclay nanocomposites over a wide range of filler loading. *Polym Int* 2008; 57: 738–743.
26. Peighambardoust SJ and Pourabbas B. Synthesis and characterization of conductive polypyrrole/montmorillonite nanocomposites via one-pot emulsion polymerization. *Macromol Symp* 2007; 247: 99–109.
27. Kim BH, Jung JH, Hong SH, et al. Physical characterization of emulsion intercalated polyaniline-clay nanocomposite. *Curr Appl Phys* 2001; 1: 112–115.
28. Samrana K, Shahzada A, Jiri P, et al. Polyaniline–sodium montmorillonite clay nanocomposites: effect of clay concentration on thermal, structural, and electrical properties. *J Mater Sci* 2012; 47: 420–428.
29. Boukerma K, Piquemal JY, Chehimi MM, et al. Synthesis and interfacial properties of montmorillonite/polypyrrole nanocomposites. *Polymer* 2006; 47: 569–576.